Directed Abelian algebras and their application to stochastic models

F. C. Alcaraz*
Instituto de Física de São Carlos, Universidade de São Paulo, Caixa Postal 369, 13560-590, São Carlos, São Paulo, Brazil

V. Rittenberg†
Physikalisches Institut, Bonn University, 53115 Bonn, Germany

(Received 7 June 2008; published 28 October 2008)

With each directed acyclic graph (this includes some D-dimensional lattices) one can associate some Abelian algebras that we call directed Abelian algebras (DAAs). On each site of the graph one attaches a generator of the algebra. These algebras depend on several parameters and are semisimple. Using any DAA, one can define a family of Hamiltonians which give the continuous time evolution of a stochastic process. The calculation of the spectra and ground-state wave functions (stationary state probability distributions) is an easy algebraic exercise. If one considers D-dimensional lattices and chooses Hamiltonians linear in the generators, in finite-size scaling the Hamiltonian spectrum is gapless with a critical dynamic exponent $z=D$. One possible application of the DAA is to sandpile models. In the paper we present this application, considering one- and two-dimensional lattices. In the one-dimensional case, when the DAA conserves the number of particles, the avalanches belong to the random walker universality class (critical exponent $\sigma_\tau=3/2$). We study the local density of particles inside large avalanches, showing a depletion of particles at the source of the avalanche and an enrichment at its end. In two dimensions we did extensive Monte-Carlo simulations and found $\sigma_\tau=1.780\pm0.005$.

DOI: 10.1103/PhysRevE.78.041126 PACS number(s): 05.50.+q, 05.65.+b, 46.65.+g, 45.70.Ht

I. INTRODUCTION

It was Dhar [1,2] who pointed out that certain Abelian algebras play an important role in understanding the properties of sandpile models. The time evolution of these systems is given, in the continuum limit, by a non-Hermitian Hamiltonian which acts nonlocally in the configuration space.

The expression for the Hamiltonian contains local generators of an Abelian algebra acting in the vector space of the regular representation of the Abelian algebra. In some cases this vector space can be identified with the recurrence states (configurations) of the sandpile models. These algebras have a special structure describing topplings from a site to its neighbors. The net result is a highly nonlocal interaction.

The Abelian algebra appears in two different ways. On the one hand, it determines the Hamiltonian that drives the system to the stationary state. On the other hand, if one considers the action of one of the generators on the stationary state of the system, the algebra describes through topplings an avalanche triggered by the local action of the generator. One can attach a virtual time to the progression of the avalanche. This is possible due to the Abelian nature of the algebras. In some cases the real and virtual times can be combined in a unique time (see [3] for an example); we are not considering this case here.

In the present paper we are going to present a large class of Abelian algebras that we call directed Abelian algebras (DAAs). They are defined as follows. One takes a directed acyclic graph [4] (these graphs are much used in mathematics and computer sciences [5]). They are formed by oriented links (edges) to which we attach arrows. There are no oriented closed loops. To each site (vertex) of that graph one attaches a generator of a DAA. There are as many relations among the generators as sites in the graph. Examples of directed acyclic graphs are some lattices in any number of dimensions. The direction in which the sandpiles propagate can be identified with the virtual time. The evolution of the avalanches can be seen as a growth process in one space dimension less [6].

The DAA are semisimple (all representations are decomposable into irreducible representations). They also have a special property: they have only one-dimensional irreducible representations and the number of nonequivalent representations coincides with the dimension of the regular representation. Since the Hamiltonians act onto the regular representations, they can be diagonalized in a trivial way. This stays true even if the Hamiltonians describe the evolution of systems in any number of dimensions. At least in some cases, all the eigenfunctions can be easily obtained.

The stationary state, which is of product measure form (no correlations), can also be obtained in any number D of dimensions. The thermodynamic limit of the spectra is also very simple.

All systems described by directed algebras are critical with the dynamic critical exponent having the value $z=D$. This does not imply that the avalanches have to be critical since they evolve in virtual time. They might have exponential tails.

The paper is organized as follows. In Sec. II we define a quadratic DAA on a one-dimensional lattice. It is a two-state model in which one has a particle or a vacancy on each site. We give the Hamiltonian which gives the time evolution of this system and show how to compute its spectrum exactly. The ground-state wave function is of product form. The average density is uniform in spite of the system being open.

*alcaraz@if.sc.usp.br
†vladimir@th.physik.uni-bonn.de

The Hamiltonian spectrum and eigenfunctions are given in Appendix A for the physically relevant case in which the number of particles is conserved.

In Sec. III we study the avalanches in the model defined in Sec. II. We show that they belong to the "random walker" universality class [7]. The probability of finding an avalanche of virtual time T corresponds to the probability of having a first passage at time T of the random walker. The connection between the present paper and the totally asymmetric Oslo model [9–11] is presented in Appendix B. We also look at the average density of particles left in the system when the avalanche stopped at time T. The density of particles is no longer uniform. Since the physical process is directed, the region near the beginning of the avalanche is depleted and the region at the end of the avalanche is enriched in particles. For long avalanches, the particle density distribution functions become singular at both ends of the avalanches. It is easy to understand the physical origin of the two singularities.

Higher-order one-dimensional DAAs are defined in Sec. IV. They correspond to N-state models. All the properties of the two-state models are recovered and no new qualitative features appear.

The construction of a DAA on an arbitrary directed acyclic graph is presented in Sec. V. As applications, we consider DAAs on a one-dimensional lattice, in which a site i is related to two successive sites $i+1$ and $i+2$, and on two-dimensional lattices. In two dimensions, one obtains avalanches belonging to the universality class described in [13–15]. We have done large-scale Monte Carlo simulations to measure the exponent σ_τ (usually denoted by τ_t). The result does not agree with the expected value $\sigma_\tau=7/4$.

Our conclusions are presented in Sec. VI.

II. A QUADRATIC DIRECTED ABELIAN ALGEBRA AND ITS APPLICATION TO A STOCHASTIC PROCESS

In this section we first show how to define the Hamiltonian describing a stochastic process by using an associative algebra. We then consider a simple application of quadratic directed Abelian algebra defined on a one-dimensional lattice. Associated with this algebra, we may define a family of stochastic processes, sharing the same stationary state.

Let us now consider an associative algebra with generators $A(i)$ $(i=1,2,\ldots,m)$. Taking products of the generators one gets the words $W(r)$. The algebra is defined by giving some relations between the words. If we can choose the linearly independent words $\{W(r);\ r=1,\ldots,n_W\}$ such that any product of them verifies the relation

$$W(r)W(s)=\sum_{q=1}^{n_W} p_q^{r,s} W(q), \quad p_q^{r,s}\geqslant 0, \quad \sum_{q=1}^{n_W} p_q^{r,s}=1, \tag{1}$$

then the Hamiltonian

$$H=\sum_{u=1}^{n_W} c(u)[1-W(u)], \tag{2}$$

acting in the vector space defined by the basis of independent words $\{W(s)\}$, is an intensity matrix provided that the coefficients $c(u)$ are nonnegative [16]. H is acting from the left on the words $W(s)$ of the vector space: $W(u)W(s)$ [$W(u)$ is one of the terms in (2) and $W(s)$ belongs to the vector space]. The action of the n_W independent words $\{W(u)\}$ on the vector space defined by the same words gives the regular representation of the algebra.

If the algebra A contains a left ideal [17] defined by the words I, the Hamiltonian (2) acting on this ideal gives again a stochastic process. If A has several ideals $I_1\subset I_2\subset\cdots\subset I_n$, H has a block triangular form. The ground-state wave function (eigenvalue equal to zero) is a linear combination of the states (words) which define the vector space I_1. These states correspond to the recurrent states. The words belonging to the ideals $I_2,\ldots,I_n$ but not belonging to I_1 do not appear in the stationary state.

One can obtain Hamiltonians describing stochastic processes using associative algebras even if the positivity conditions (1) are not satisfied. This can be achieved by working not in the regular representation of the algebra but in other representations. The following simple example illustrates the procedure.

Consider the quadratic algebra with only one generator a:

$$a^2=(1-\mu)a+\mu e, \quad e^2=e, \quad ea=ae, \tag{3}$$

and

$$H=1-a, \tag{4}$$

where μ is a parameter. If $0\leqslant\mu\leqslant 1$, the condition (1) is satisfied. H is an intensity matrix

$$H=\left(\begin{array}{c|cc} & e & a \\ \hline e & 1 & -\mu \\ a & -1 & \mu \end{array}\right), \tag{5}$$

where e is the 2×2 unit matrix. Let us now perform the similarity transformation

$$H'=SHS^{-1}, \tag{6}$$

where

$$S=\begin{pmatrix} 1 & \xi \\ \xi & 1 \end{pmatrix}$$

and $\xi=(1-\alpha)/(1-\beta)$. H' is

$$H'=\begin{pmatrix} \alpha & -\beta \\ -\alpha & \beta \end{pmatrix}. \tag{7}$$

The algebra (3) stays unchanged with $\mu=\alpha+\beta-1$. The matrix (7) is the most general 2×2 intensity matrix $(0\leqslant\alpha,\ \beta\leqslant 1)$. Notice that the physical process depends on two parameters instead of one [which appears in the algebra (3)] and that the range of μ has changed: $-1<\mu\leqslant 1$.

The probabilities $P_q(t)$ of finding the words $W(q)$ at the time t can be obtained from the master equation

$$\frac{d}{dt}P(t)=-HP(t), \tag{8}$$

where

$$P(t) = \sum_{q=1}^{n_W} P_q(t) W(q). \tag{9}$$

We now apply this formalism to a simple example of a quadratic DAA (for applications to non-Abelian algebras, see [16]). Consider a one-dimensional lattice with L sites. We attach to each site i $(i=1,2,\ldots,L)$ a generator a_i. A quadratic DAA is defined by the relations

$$a_i^2 = p_1 a_{i+1}^2 + p_2 a_{i+1} + p_3 + q_1 a_i a_{i+1} + q_2 a_i, \tag{10}$$

for $i=1,2,\ldots,L-1$,

$$a_L^2 = \mu + (1-\mu) a_L, \tag{11}$$

$$[a_i, a_j] = 0, \quad i,j = 1,2,\ldots,L, \tag{12}$$

where p_m and q_n are the probabilities, and

$$\mu = p_1 + p_2 + p_3, \quad 1-\mu = q_1 + q_2. \tag{13}$$

Notice that the words with a given value i are related to words with values $j>i$, therefore we have a preferred direction on the lattice. The relation (11) was obtained by taking $a_{L+1}=1$ in Eq. (10).

The 2^L monomials $1, a_1, \ldots, a_L, a_1 a_2, \ldots, a_{L-1} a_L, \ldots, a_1 a_2 \cdots a_L$, are the independent words of the DAA (they define the regular representations of the DAA). One can check, using (10)–(13), that the relations (1) are verified. The DAA (10)–(12) can therefore be used to define a family of stochastic processes whose Hamiltonians are obtained by arbitrary choices of $c(u)$ $(u=1,\ldots,2^L)$ in (2). If $\mu=0$, the algebra (10)–(13) has an ideal

$$I_1 = a_1 a_2 \cdots a_L, \tag{14}$$

which gives in the regular representation an absorbing state in the stochastic process defined by (2).

One can map the vector space of the regular representation onto a lattice with L sites. On each site i one has a particle if a_i appears in the monomial or a vacancy if a_i does not appear in the monomial. With the word "1" one associates the empty lattice. There are 2^L configurations obtained in this way.

The a_i $(i=1,2,\ldots,L)$ acting on the regular representation are not in the diagonal form. They can, however, be diagonalized simultaneously, and one obtains in this way 2^L one-dimensional irreducible representations of the algebra. The eigenvalues of a_i, denoted by x_i, can be obtained recursively using the distinct eigenvalues x_{i+1} of a_{i+1},

$$x_L = 1, \mu,$$

$$x_i^2 - x_i(q_1 x_{i+1} + q_2) - (p_1 x_{i+1}^2 + p_2 x_{i+1} + p_3) = 0,$$

where $i=L-1, L-2, \ldots, 1$.

Notice that one has to solve only quadratic equations and that the a_i have a common eigenvalue $x_i=1$. One can easily find the corresponding eigenfunction in the regular representation:

$$a_i \Phi = \Phi, \quad i = 1,2,\ldots,L. \tag{15}$$

The expression for Φ is

$$\Phi = \prod_{i=1}^{L} \frac{\mu + a_i}{1+\mu}. \tag{16}$$

In the expression for Φ there is only the parameter μ instead of the four parameters appearing in (10). The proof is straightforward. We have

$$a_L \frac{\mu + a_L}{1+\mu} = \frac{\mu + a_L}{1+\mu}, \tag{17}$$

where we have used (11). We now use (10) and (17) to obtain

$$a_{L-1} \frac{\mu + a_{L-1}}{1+\mu} \frac{\mu + a_L}{1+\mu} = \frac{\mu + a_{L-1}}{1+\mu} \frac{\mu + a_L}{1+\mu} \tag{18}$$

and repeat the procedure to get, due to (12),

$$a_i \Phi = \Phi, \quad i = L-2, \ldots, 1. \tag{19}$$

The eigenstate Φ, due to (15), gives the stationary state for the arbitrary stochastic models defined by (2), i.e., $H\Phi=0$. The average density in the stationary state (16) is equal to $1/(1+\mu)$ and varies between $1/2$ and 1.

Other equivalent representations of the algebra (10) can be used to describe stochastic processes. In Appendix B we give two examples. One of them is the totally asymmetric Oslo model [9–11].

We now consider the simple stochastic process given by the Hamiltonian

$$H = \sum_{i=1}^{L} (1 - a_i)/L. \tag{20}$$

The physical interpretation of the stochastic process described by (20) can be more easily understood using the configuration space and discrete times. At the time t one takes a configuration with a certain distribution of particles on the L sites (not more than one per site). With probability $1/L$ a particle is added at the site i. If the site is empty, the particle stays at i. If one has a particle at i already, one obtains several configurations with a probability given by the toppling rules given by the DAA (10). Notice that the stationary state is of product form and therefore there are no correlations in the stationary state.

To compute the spectrum of H, we can take all the a_i in their diagonal representation. Since H acts in the regular representation, all the irreducible one-dimensional representations (irreps) of the DAA have to appear. The number of irreps coincides with the dimension of the vector space given by the regular representation. Therefore, each representation appears only once and the calculation of the spectrum is trivial (see Appendix A). It is interesting to compute the energy gap of H. The ground-state energy is zero. The first excited state is obtained by taking $a_i=1$ $(i=L, L-1, \ldots, 2)$. It follows from (10) that a_1 can take two values: 1 and $-\mu$. One obtains two one-dimensional representations. The first one is the ground state with energy zero and the second one corresponds to the first excited state with energy $E_1=(1+\mu)/L$

(we call the eigenvalues of H energies). The dynamic critical exponent z is defined by the relation $\lim_{L\to\infty} L^z E = \text{const}$. Since in our case

$$\lim_{L\to\infty} LE_1 = 1 + \mu, \tag{21}$$

it follows that $z=1$. This result is interesting for several reasons. The value $z=1$ is also obtained when the system is conformally invariant [16]. This is certainly not the case here since there are no correlations in the stationary state. The finite-size scaling limit of the spectra can be changed [through a change of the parameters in (10)] almost arbitrarily and are not described by representations of the Virasoro algebra as expected in a conformally invariant theory. The result is not surprising since, in the configuration space, each a_i acts through topplings in a highly nonlocal way and there is no reason to expect conformal invariance. It is nice to have an example that illustrates this phenomenon in full generality.

There is another interesting consequence of (21). Since the energy gap in the thermodynamic limit vanishes, the system is critical. Does this imply that the avalanches, to be discussed later, are described always by power laws as expected by self-organized criticality (SOC)? The answer is no. As one can see from (10), unless all the coefficients p_2, p_3, and q_2 vanish, the number of particles is not conserved; particles are lost and no particles are added to the system. One expects therefore an exponential decay for the probability of having an avalanche of a certain size [18,19]. For avalanches that are critical one defines a dynamic critical exponent z_a [20] related to the virtual time at which the avalanche occurs. It is not clear to us why the two exponents z and z_a should coincide, although in many examples they do.

The spectrum and eigenfunctions of H are given in Appendix A for the simpler case in which one conserves the number of particles in (10). The knowledge of the spectra allows us to get information about time-dependent quantities. If one starts, for example, with an empty lattice, one can look at the time dependence of the average density which, in the large-L limit, should algebraically reach its value in the stationary state.

There is a purely algebraic way to compute the density for finite L. Let us assume that at $t=0$ we start with an empty lattice. This corresponds to the word "1" in the algebra. In the basis of monomials [see (9)], one has

$$P(t) = e^{-Ht} \times 1 = e^{-Ht}. \tag{22}$$

After expanding the exponential in (22) we use the algebra (10)) and express $P(t)$ in terms of monomials. We take $a_i=y$ (for all i's) and obtain the function $P(t,y)$. The density is given by the expression

$$\rho(t) = \left.\frac{dP(t,y)}{dy}\right|_{y=1}. \tag{23}$$

Let us observe that we can take the parameters in (10) and (11) as i dependent, the ground-state wave function maintaining the product form

$$\Phi = \prod_{i=1}^{L} \frac{\mu_i + a_i}{1+\mu_i}, \tag{24}$$

where the definition of μ_i is obvious. The dynamic critical exponent z stays unchanged.

III. A QUADRATIC DIRECTED ABELIAN ALGEBRA AND AVALANCHES

In the last section we discussed the time evolution of a system described by H given by (20). In order to study its spectrum and obtain the ground-state wave function, we have used the quadratic DAA (10)–(13). From these results, in this section, we need only the expression (23) to use the DAA to study avalanches. To simplify the calculation we consider the case in which the number of particles is conserved. In this case, the relations (10) take the form

$$a_i^2 = \mu a_{i+1}^2 + (1-\mu) a_i a_{i+1}. \tag{25}$$

The physical meaning of (25) is simple: if one has two particles on the site i, with probability μ they reach the site $i+1$ and with probability $(1-\mu)$ one particle moves to the site $i+1$ and one stays at the site i. Multiplying (25) by a power of a_i, we can find the probabilities that n particles on site i move in a block onto the site $i+1$ or only $n-1$ particles move and one stays at the site i. Obviously, the number of particles is not conserved at the end of the system.

To examine avalanches in our system, we take the stationary state given by (16) and consider only the configurations in which the first site is occupied [they have a probability $1/(1+\mu)$]. We add one particle on the first site and analyze the consequences. The overall effect of adding the particle is trivial to derive:

$$a_1^2 \prod_{i=2}^{L} \frac{\mu + a_i}{1+\mu} = [\mu + (1-\mu)a_1] \prod_{i=2}^{L} \frac{\mu + a_i}{1+\mu}, \tag{26}$$

where we have used (15) and (16). This tells us that the changes take place only at the first site. With probability μ it becomes empty and with probability $(1-\mu)$ it is occupied by a particle.

We are interested in more detailed properties of this process. First, we would like to know the probability $p(k)$ for the first k sites to be affected by the action of a_1^2 and the remaining $L-k$ sites untouched (this defines an avalanche of size k, starting at the first site). The physics inside an avalanche is easy to understand by looking at (25). Particles close to the origin of the avalanche are pushed toward its end. We will be interested therefore to obtain the nonhomogeneous density of particles inside an avalanche. Let us first obtain $p(k)$.

We use (25) and obtain

$$a_1^2 \prod_{i=2}^{L} \frac{\mu + a_i}{1+\mu} = \left(\frac{\mu(1-\mu)a_1 a_2}{1+\mu} + \frac{\mu a_2^3 + \mu^2 a_2^2 + (1-\mu)a_1 a_2^2}{1+\mu} \right) \times \prod_{i=3}^{L} \frac{\mu + a_i}{1+\mu}. \tag{27}$$

One can see that we have obtained an avalanche given by

$a_1 a_2$ of size 2 (the first two sites occupied) with probability $\mu(1-\mu)/(1+\mu)$. If we are not interested in the content of the avalanche, but only in its size, we can formally take $a_1=1$ in the right-hand side of (27), substitute the symbol=by$\hat{=}$, and get

$$a_1^2 \prod_{i=2}^{L} \frac{\mu + a_i}{1+\mu} \hat{=} \frac{\mu(1-\mu)a_2 + (1-\mu+\mu^2)a_2^2 + \mu a_2^3}{1+\mu} \times \prod_{i=3}^{L} \frac{\mu + a_i}{1+\mu}. \tag{28}$$

If we want to proceed further and compute the probabilities of larger avalanches, we have to compute quantities like

$$a_i^n \frac{\mu + a_i}{1+\mu} = \frac{1}{1+\mu}[B_0^{(n)} a_{i+1}^{n+1} + (C_1^{(n)} a_i + C_0^{(n)}) a_{i+1}^n + D_1^{(n)} a_i a_{i+1}^{n-1}], \tag{29}$$

in which we have taken into account the fact that the algebra (25) conserves the number of particles. Multiplying (29) by a_i, one obtains the recurrence relations

$$B_0^{(n+1)} = \mu C_1^{(n)}, \quad C_1^{(n+1)} = B_0^{(n)} + (1-\mu) C_1^{(n)},$$

$$C_0^{(n+1)} = \mu D_1^{(n)}, \quad D_1^{(n+1)} = C_0^{(n)} + (1-\mu) D_1^{(n)}, \tag{30}$$

with

$$C_1^{(0)} = 1, \quad D_1^{(0)} = 0, \quad C_1^{(1)} = 1-\mu, \quad D_1^{(1)} = \mu. \tag{31}$$

From this, we get

$$D_1^{(n)} = \mu C_1^{(n-1)} \tag{32}$$

and

$$C_1^{(n+1)} - C_1^{(n)} = -\mu (C_1^{(n)} - C_1^{(n-1)}). \tag{33}$$

The solution of the recurrence relation (33) is

$$C_1^{(n)} = \frac{1-(-\mu)^{n+1}}{1+\mu}. \tag{34}$$

In order to look for avalanches, in (29) one takes $a_i=1$ and, using (30) and (32), one obtains

$$a_i^n \frac{\mu + a_i}{1+\mu} \hat{=} \frac{1}{1+\mu}[\mu C_1^{(n-1)} a_{i+1}^{n+1} + (C_1^{(n)} + \mu^2 C_1^{(n-2)}) a_{i+1}^n + \mu C_1^{(n-1)} a_{i+1}^{n-1}]. \tag{35}$$

If $\mu \neq 1$ (for $\mu=1$ the process is deterministic and the two particles on site 1 move to site L where they leave the system) from (34) one can see that, for large values of n, $C_1^{(n)}$ becomes independent of n and equal to $1/(1+\mu)$. Substituting this result in (35) one obtains

$$a_i^n \frac{\mu + a_i}{1+\mu} \hat{=} \frac{1}{(1+\mu)^2}[\mu a_{i+1}^{n+1} + (1+\mu^2) a_{i+1}^n + \mu a_{i+1}^{n-1}]. \tag{36}$$

One could have obtained this last equation without solving the recurrence relations (31)–(33) (we are going to use this method in the next section). Equation (33) has an n-independent solution $C_1^{(n)}=C$. We introduce this solution in (35) and ask for the sum of the coefficients to be equal to 1. This gives $C=1/(1+\mu)$.

The whole virtual time evolution ($\tau \geqslant 1$) of the avalanches is given by the following expression:

$$a_1^2 \prod_{i=2}^{L} \frac{\mu + a_i}{1+\mu} \hat{=} \sum_{n=1}^{\tau} P_n(\tau) a_\tau^n \prod_{j=\tau+1}^{L} \frac{\mu + a_j}{1+\mu}, \tag{37}$$

where $P_n(\tau)$ is the probability that at virtual time τ an avalanche, with n particles at site $i=\tau$, is taking place. These probabilities, from (25) and (35), satisfy the recurrence relations

$$P_1(\tau) = P_2(\tau-1) R_-^{(2)},$$

$$P_2(\tau) = P_2(\tau-1) R_0^{(2)} + P_3(\tau-1) R_-^{(3)},$$

$$P_n(\tau) = P_{n+1}(\tau-1) R_-^{(n+1)} + P_n(\tau-1) R_0^{(n)} + P_{n-1}(\tau-1) R_+^{(n-1)} \tag{38}$$

for $2 \leqslant n \leqslant \tau$, with

$$P_n(1) = \delta_{n,2}, \tag{39}$$

and

$$R_+^{(n)} = \frac{f^{(n-1)}}{1+\mu}, \quad R_-^{(n)} = \mu \frac{1-f^{(n-1)}}{1+\mu},$$

$$R_0^{(n)} = 1 - R_+^{(n)} - R_-^{(n)}, \quad f^{(n)} = \frac{\mu + (-\mu)^{n+1}}{1+\mu}. \tag{40}$$

We can visualize these last equations in the following way. We take two coordinates, the virtual time τ (discrtized values) as the horizontal axis and a coordinate n (discritized values) as the vertical axis. Equation (37) describes a random walker which at time τ is at the position n, and moves to the positions $n+1$, $n-1$ or stays at n with probabilities that are n dependent. The probability of having an avalanche of size k is given by the first passage at virtual time $\tau=T=k$ to return to its initial position $x=1$, and is given by $p(\tau)=P_1(\tau)$. This probability is not simple to calculate due to the n dependence of the random walk parameters $R_-^{(n)}$, $R_0^{(n)}$, and $R_+^{(n)}$ in (38). However, the large-size avalanches are dominated by random walks that stay mostly at large distances from the origin (n large). We take $f^{(n)}=\mu/(1+\mu)$ in (40) and obtain

$$R_+^{(n)} = R_-^{(n)} = R = \mu/(1+\mu)^2, \quad R_0^{(n)} = 1 - 2R = \frac{1+\mu^2}{(1+\mu)^2}. \tag{41}$$

With probability $\mu/(1+\mu)^2$, the walker moves to $n+1$ or $n-1$ and with probability $(1+\mu^2)/(1+\mu)^2$ stays at n. In the continuum, one obtains the diffusion equation with a diffusion constant $D=\mu/(1+\mu)^2$. Consequently, the probability of having large avalanches of size k corresponds to the usual first passage time at $\tau=T=k$ [18],

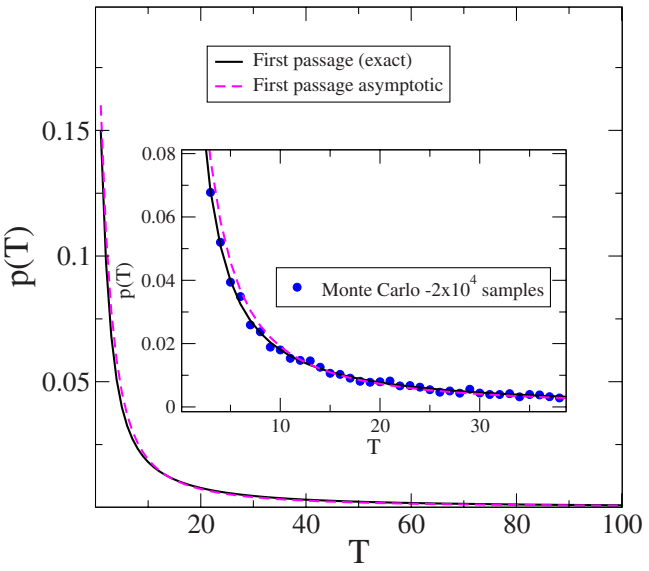

FIG. 1. (Color online) Probability distribution of avalanches of size T for the stochastic model defined by (20) and (25), with $\mu=1/4$. The exact results (black continuous line) are compared with the results (red dashed line) derived by using the asymptotic behavior of the recurrence relations (41) in (38). In the inset (blue dots) we also show, for comparison, the results obtained from a Monte Carlo simulation.

$$p(T) = P_1(T) \sim \frac{1}{\sqrt{DT^3}}. \tag{42}$$

If one defines the exponent σ_τ by the relation $p(T) \approx 1/T^{\sigma_\tau}$, where T is the duration of the avalanche, one obtains $\sigma_\tau = 3/2$. The approximation (41) for the probabilities (40) is valid if $n \gg 1/|\ln \mu|$. Since n is of the order of $\sqrt{T}$, we conclude that one can see the avalanches described by the power law (42) for

$$T \gg T_c = 1/(\ln \mu)^2. \tag{43}$$

In order to illustrate the approximation (41) we compare in Fig. 1 the results obtained by the exact recurrence relations with $\mu=1/4$ (38) (black continuum curve) with the one obtained by using the asymptotic relations (41) (red dashed curve). In the inset we show only the probabilities for relatively small avalanches ($\tau<50$), where the curves show a more pronounced difference ($T_c=1$ in this case). We also show (blue dots), for comparison, the average results obtained from 2×10^4 samples in a Monte Carlo simulation.

Having in mind applications to two-dimensional systems (see Sec. V) we are interested to know how large the avalanches need to be for a good estimate for σ_τ. We consider the quantity

$$\sigma_\tau(T) = T\frac{p(T) - p(T+1)}{p(T)}, \tag{44}$$

which is an estimate for σ_τ. In Fig. 2 we show the values of $\sigma_\tau(T)$ for $\mu=0.99$ ($T_c=9900$ in this case). We observe that $\sigma_\tau(T)$ first increases with T, giving a maximum value of 1.91, and then decreases. Notice that even by taking very large avalanches one still gets a poor estimate: $\sigma_\tau(10^6) = 1.5445$. This estimate is larger than the expected value 1.5. Using extrapolation techniques (eight-degree polynomial fitting) we can improve the estimate substantially and get $\sigma_\tau = 1.5006 \pm 0.0008$. We have to stress that for $p(T)$ we have used exact results and not Monte Carlo simulations as in Sec. V.

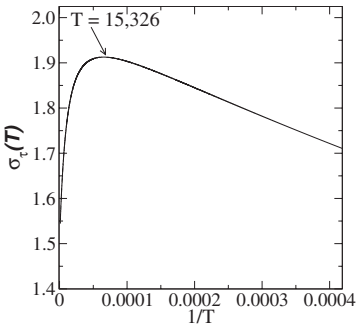

FIG. 2. Estimate $\sigma_\tau(T)$ defined in (44) for $\mu=0.99$ and $2400 < T < 10^6$. The estimate increases, with T, up to $T=15\,326$. The last value of the estimate is $\sigma_\tau(10^6)=1.5445$.

If μ is small, the estimates of $\sigma_\tau(T)$ improve dramatically. In Fig. 3 we show $\sigma_\tau(T)$ for $\mu=0.1$ (T_c is negligible in this case).

We observe that, in contrast with the case $\mu=0.99$, the estimates increase with T and one can get a very good precision for relatively small values of T. A best fit to the data gives

$$p(T) = A/T^g + B/T^h, \tag{45}$$

where $A=1.0794\pm0.0003$, $B=-7.16\pm0.05$, $g = 1.500\,00 \pm 0.000\,01$, and $h=2.448\pm0.003$.

In this way one has obtained a concrete realization of the model of Maslov and Zhang [7] in which $z_a=1$. The same result was obtained in a different context. A generalized totally asymmetric hopping processes on a ring (fixed density of particles) was considered [21]. More than one particle per site is allowed. The rules of the hopping processes are fixed by the condition of integrability of the system (one can write the Bethe ansatz). Interestingly enough, the rules coincide with those obtained from the DAA (25). There is no relation (11) on a ring. If the density of particles on the ring is equal

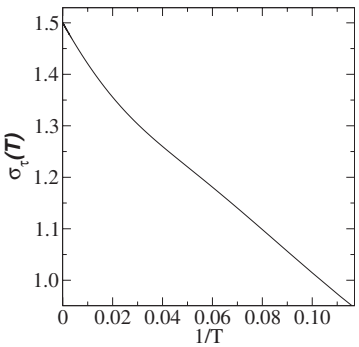

FIG. 3. Estimate $\sigma_\tau(T)$ defined in (44) for $\mu=0.1$ and $1 < T < 10^6$. The last value of the estimate is $\sigma_\tau(10^6)=1.499\,99$.

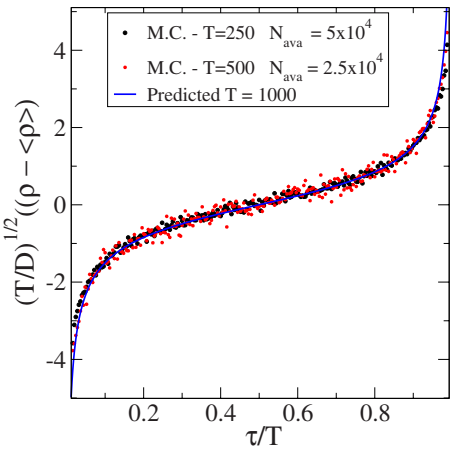

FIG. 4. (Color online) Depletion and enrichment of particles in avalanches of different sizes T. $(T/D)^{1/2}[\rho(\tau,T)-\langle\rho\rangle]$ as a function of τ/T obtained from Monte Carlo simulations for $T=250$ and 500. The numbers of avalanches N_{ava} observed in each case are given in the inset. The solid curve is the result of the calculation using (48) and (49) for $T=1000$.

to the average density $1/(1+\mu)$ obtained in our model, the two models describe the same large avalanches.

We would like to make the connection between our approach and the work of Stapleton and Christensen on the totally asymmetric Oslo model (TAOM) and its generalizations[11], where similar results were obtained. As shown in detail in Appendix B in the case of the two-state model, in the TAOM one takes another representation (not the regular one) of the same algebra (25). This representation depends on two parameters, whereas the algebra depends only on one. The same picture stays valid for the multistate one-dimensional models discussed in Sec. IV. We have shown in a straightforward way the correspondence to the random walker process and proceeded by deriving the probability distribution of avalanches. In [11] the authors computed moments of the toppling probability distribution and came to the same conclusion.

Up to now we were interested in the probability of having an avalanche of size T. We would like to know the physics of a given avalanche. It is useful to visualize the virtual time τ as either a time coordinate or a space coordinate.

As a result of the DAA (25), particles present in the stationary state [average density $\langle\rho\rangle=1/(1+\mu)$] are pushed away from the origin of the avalanche toward its end. For a given avalanche of size T, we consider the quantity $\rho(\tau,T)-\langle\rho\rangle$, where $\rho(\tau,T)$ is the average density at virtual time τ. In order to compute this quantity we could use (29) without taking $a_i=1$. This is a lengthy calculation. Instead we did Monte Carlo simulations. In Fig. 4, for $\mu=1/2$ we show $(\rho(\tau,T)-\langle\rho\rangle)$ multiplied by $\sqrt{T/D}$ as a function of τ/T for three avalanche sizes. The function is antisymmetric. D is the diffusion constant $[D=\mu/(1+\mu)^2]$. We notice not only a nice data collapse but a singular depletion of particles for small values of τ/T and a singular enrichment of particles for τ/T close to 1. We have done similar simulations for other values of μ, and the data fall on top of those shown for $\mu=1/2$. If one looks at τ as a space coordinate, one gets what one would expect to see in the aftermath of an avalanche. For small values of τ/T one finds

$$\rho-\langle\rho\rangle\sim-\frac{c}{4}\left(\frac{D}{\tau}\right)^{1/2} \tag{46}$$

where $c\sim0.56$.

Theoretically one can obtain the scaling function which describes the data shown in Fig. 4 in the following way. We use the random walker approximation. Let $P(x,\tau;T)=P(x,T-\tau;T)$ be the conditional probability to find a random walker at time $0<\tau<T$ at the position x if the first passage time is T. This is a Brownian excursion [8]. The average position at time τ is

$$\langle x\rangle_{\tau,T}=\int_0^\tau xP(x,\tau;T)dx. \tag{47}$$

One can compute

$$\rho(\tau,T)-\langle\rho\rangle=-\frac{1}{2}\frac{d}{d\tau}\langle x\rangle_{\tau,T}. \tag{48}$$

In order to do the calculation we have used the lattice expression $P(x,\tau;T)$ obtained in the simpler case in which the random walker that is at the position x at time τ moves to $x+1$ or $x-1$ with probabilities $1/2$ at $\tau+1$. The random walker starts at $x=0$ at time $\tau=0$ and returns to $x=0$ at $\tau=T$ (T even). One has [22]

$$P(x,\tau;T)=\frac{x^2T}{2}\frac{[(T/2-1)!]^2}{(T-2)!}\times\frac{(\tau-1)!(T-\tau-1)!}{\left(\frac{\tau-x}{2}\right)!\left(\frac{\tau+x}{2}\right)!\left(\frac{T-\tau-x}{2}\right)!\left(\frac{T-\tau+x}{2}\right)!}. \tag{49}$$

Note that in the continuum the diffusion constant is $D=1/2$ in this case. The function $P(x,\tau;T)$ satisfies various scaling laws. In particular, if we take $\tau=T/2$, it scales as shown in Fig. 5. A consequence of this scaling behavior is that

$$\langle x\rangle_{T/2,T}\sim T^{1/2}. \tag{50}$$

For $\tau=T/2$, $\langle x\rangle_{\tau,T}$ has its maximum value. We have checked a more general scaling property:

$$\langle x\rangle_{\tau,T}=\sqrt{DT}f(\tau/T). \tag{51}$$

Obviously $D=1/2$ in the present case.

For small values of τ, one gets

$$\langle x\rangle_{\tau,T}\sim c\sqrt{D\tau}, \tag{52}$$

where $c\sim0.56$. The expression (52) is what one expects for a random walker. The constant c appears from the constraint $x>0$. If we use (48) and (52) we get (46); therefore the singularity observed at small values of τ has a simple explanation.

We have computed $\langle x\rangle_{\tau,T}$ and used (48) with $T=1000$ to obtain the solid curve shown in Fig. 4.

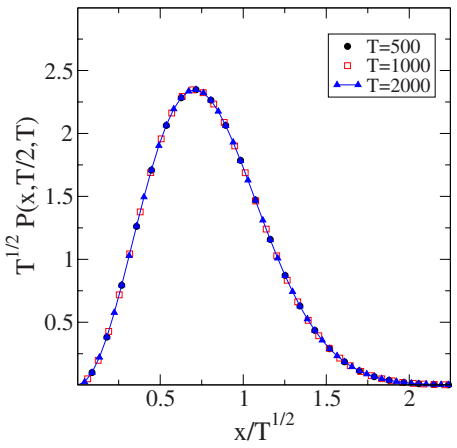

FIG. 5. (Color online) Conditional probability function $P(x,T/2;T)$ multiplied by $T^{1/2}$ as a function of $x/T^{1/2}$ for $T=500$, 1000, and 2000.

IV. HIGHER-ORDER ONE-DIMENSIONAL DIRECTED ABELIAN ALGEBRAS

The quadratic DAA discussed in the previous section can be generalized to higher orders. These algebras define stochastic models with recurrence states (stable configurations) containing at most $N-1$ particles per site. As we are going to see all the results obtained for the quadratic case generalize in a trivial way. The order-N DAA with conservation of the number of particles is defined as follows:

$$a_i^N = \sum_{k=0}^{N-1} \alpha_k a_i^k a_{i+1}^{N-k} \quad (i=1,\ldots,L-1), \tag{53}$$

$$a_L^N = \sum_{k=0}^{N-1} \alpha_k a_L^k, \tag{54}$$

$$\sum_{k=0}^{N-1} \alpha_k = 1, \quad 0 \leqslant \alpha_k \leqslant 1. \tag{55}$$

One recovers the case $N=2$, taking $\alpha_0=\mu$. The stationary states Φ of the family of Hamiltonians [see (2)] associated with these algebras, i.e.,

$$a_i \Phi = 1, \tag{56}$$

have the expression

$$\Phi = \prod_{i=1}^{L} \frac{\sum_{m=0}^{N-1} \beta_m a_i^m}{N - \sum_{s=1}^{N-1} s\alpha_s}, \tag{57}$$

where

$$\beta_m = \sum_{k=0}^{m} \alpha_k. \tag{58}$$

The average density

$$\rho = \frac{\sum_{m=1}^{N-1} m\beta_m}{N - \sum_{s=1}^{N-1} s\alpha_s} \tag{59}$$

varies between $(N-1)/2$ and $N-1$.

The algebra (53) has N^L one-dimensional representations. As in Sec. II we restrict ourselves to the simple Hamiltonian (20). Its eigenspectrum can be obtained in the same way as for the $N=2$ case. As compared with the case $N=2$ one has to solve Nth-order algebraic equations instead of quadratic ones. The dynamic critical exponent stays unchanged, $z=1$.

We present the study of avalanches for the case $N=3$ only. The generalization to other values of N will become obvious.

We take α_0 and α_1 as the parameters of the algebra. Using (57) we have

$$\Phi = \prod_{i=1}^{L} \frac{a_i^2 + (\alpha_0+\alpha_1)a_i + \alpha_0}{1+2\alpha_0+\alpha_1}. \tag{60}$$

We consider only configurations in which on the first site we have two particles and add one more particle on this site. As in the case $N=2$, we have to compute the quantity

$$\begin{aligned} a_i^n \frac{a_i^2 + (\alpha_0+\alpha_1)a_i + \alpha_0}{1+2\alpha_0+\alpha_1} &= (1+2\alpha_0+\alpha_1)^{-1} \times [A_0^{(n)} a_{i+1}^{n+2} + (B_1^{(n)} a_i + B_0^{(n)}) a_{i+1}^{n+1} \\ &+ (C_2^{(n)} a_i^2 + C_1^{(n)} a_i + C_0^{(n)}) a_{i+1}^n + (D_2^{(n)} a_i^2 + D_1^{(n)} a_i) a_{i+1}^{n-1} \\ &+ E_2^{(n)} a_i^2 a_{i+1}^{n-2}]. \end{aligned} \tag{61}$$

Multiplying (61) by a_i, one obtains the following recurrence relations, valid for $n \geqslant 2$:

$$\begin{aligned} C_2^{(n+1)} - C_2^{(n)} &= -\alpha_0 (C_2^{(n)} - C_2^{(n-2)}) - \alpha_1 (C_2^{(n)} - C_2^{(n-1)}), \\ D_2^{(n+1)} - D_2^{(n)} &= -\alpha_0 (D_2^{(n)} - D_2^{(n-2)}) - \alpha_1 (D_2^{(n)} - D_2^{(n-1)}), \\ E_2^{(n+1)} - E_2^{(n)} &= -\alpha_0 (E_2^{(n)} - E_2^{(n-2)}) - \alpha_1 (E_2^{(n)} - E_2^{(n-1)}), \end{aligned} \tag{62}$$

$$\begin{aligned} A_0^{(n+1)} &= \alpha_0 C_2^{(n)}, \quad B_1^{(n+1)} = \alpha_1 C_2^{(n)} + \alpha_0 C_2^{(n-1)}, \\ B_0^{(n+1)} &= \alpha_0 D_2^{(n)}, \quad C_1^{(n+1)} = \alpha_1 D_2^{(n)} + \alpha_0 D_2^{(n-1)}, \\ C_0^{(n+1)} &= \alpha_0 E_2^{(n)}, \quad D_1^{(n+1)} = \alpha_1 E_2^{(n)} + \alpha_0 E_2^{(n-1)}, \end{aligned} \tag{63}$$

with

$$\begin{aligned} C_2^{(2)} &= \frac{1}{1+2\alpha_0+\alpha_1}, \quad D_2^{(2)} = \frac{\alpha_0+\alpha_1}{1+2\alpha_0+\alpha_1}, \\ E_2^{(2)} &= \frac{\alpha_0}{1+2\alpha_0+\alpha_1}, \quad C_2^{(1)} = D_2^{(1)} = E_2^{(1)} = 0. \end{aligned} \tag{64}$$

From (62)–(64) we obtain

$$D_2^{(n)} = (\alpha_0+\alpha_1) C_2^{(n)}, \quad E_2^{(n)} = \alpha_0 C_2^{(n)}. \tag{65}$$

We notice that (65) has n-independent solutions valid for large n:

$$C_2^{(n)} = C. \tag{66}$$

This implies [see (63)]

$$A_0^{(n)} = \alpha_0 C, \quad B_0^{(n)} = \alpha_0(\alpha_0 + \alpha_1)C, \quad C_0^{(n)} = \alpha_0^2 C,$$

$$B_1^{(n)} = (\alpha_0 + \alpha_1)C, \quad C_1^{(n)} = (\alpha_0 + \alpha_1)^2 C,$$

$$D_1^{(n)} = \alpha_0(\alpha_0 + \alpha_1)C. \tag{67}$$

If we are not interested in what happens in the avalanche on site i, we take $a_i=1$ in (61). We substitute the coefficients in (61) by (65)–(67) and fix the value of $C=(1+2\alpha_0+\alpha_1)^{-1}$ by requiring that the sum of the coefficients is equal to 1. We obtain

$$a_i^n \frac{a_i^2 + (\alpha_0 + \alpha_1)a_i + \alpha_0}{1 + 2\alpha_0 + \alpha_1}$$
$$\triangleq (1 + 2\alpha_0 + \alpha_1)^{-2} \times [\alpha_0 a_{i+1}^{n+2} + (\alpha_0 + \alpha_1)(1 + \alpha_0)a_{i+1}^{n+1}$$
$$+ (1 + \alpha_0^2 + (\alpha_0 + \alpha_1)^2))a_{i+1}^n + (\alpha_0 + \alpha_1)(1 + \alpha_0)a_{i+1}^{n-1}$$
$$+ \alpha_0 a_{i+1}^{n-2}]. \tag{68}$$

This can be interpreted as a random walker that moves in a symmetric way one and two steps up and down. We are therefore back to the Maslov-Zhang [7] universality class.

V. DIRECTED ABELIAN ALGEBRAS IN VARIOUS GEOMETRIES

Up to now we have considered DAAs on a one-dimensional lattice. DAAs can be generalized to more dimensions and different lattices. For simplicity, in this section, we confine ourselves to quadratic DAAs which conserve the number of particles.

We divide the sites of a graph into two sets: bulk and boundary sites. Take a bulk site b on the lattice and join it by outgoing arrows to the sites $i(i=1,2,\ldots,M)$ (see Fig. 6). With each of the $M+1$ sites one associates a generator a_i. A quadratic directed relation can be associated with the site b:

$$a_b^2 = \sum_{k=1}^{M} (\alpha_k a_k^2 + \beta_k a_b a_k) + \sum_{k=1}^{M} \sum_{l=k+1}^{M} \gamma_{k,l} a_k a_l. \tag{69}$$

We denote

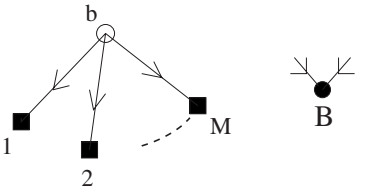

FIG. 6. The bulk site b is connected with the sites $1,2,\ldots,M$. Bulk sites are denoted by empty circles and boundary sites B by filled circles. Squares denote sites that can be of bulk or boundary type.

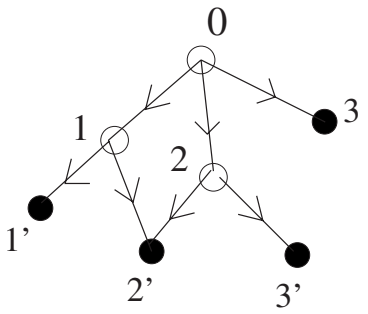

FIG. 7. Example of a directed acyclic graph, where the empty (filled) circles are bulk (boundary) sites.

$$\mu = \sum_{k=1}^{N} \alpha_k + \sum_{k=1}^{M} \sum_{l=k+1}^{M} \gamma_{k,l} = 1 - \sum_{k=1}^{N} \beta_k, \tag{70}$$

where $0<\mu\leqslant 1$. With a boundary (sink) site B (no outgoing arrows) one associates a generator a_B satisfying the relation

$$a_B^2 = \mu + (1 - \mu)a_B. \tag{71}$$

The sites $i=1,2,\ldots,M$ can be bulk or boundary sites with which we associate relations like (69) or (71), respectively (see Fig. 7). There are as many relations as sites. The graph starts with bulk sites and ends with boundary sites. This is a directed acyclic graph [5].

We call a lattice $\mathcal{L}$ on which one can define a DAA a directed acyclic lattice. The DAA is defined by the $\mathcal{L}$ relations (69) and (71). The algebra has $2^{\mathcal{L}}$ one-dimensional irreducible representations and the regular representation is $2^{\mathcal{L}}$ dimensional. Examples of two-dimensional (2D) directed acyclic lattices are shown in Fig. 8. If we are interested in critical exponents we have to consider well-defined sequences of larger and larger graphs.

One can show that for any directed acyclic lattice one has

$$a_I \Phi = \Phi, \quad I \in \mathcal{L}, \tag{72}$$

where I is any site of the lattice and

$$\Phi = \prod_{J \in \mathcal{L}} \frac{\mu + a_J}{1 + \mu}. \tag{73}$$

I and J are all the sites of the directed acyclic lattice with $\mathcal{L}$ sites. The proof is by finite induction, similar to the one used for the one-dimensional case. One starts with the boundary generators and finishes with the bulk generators attached to sites with no incoming arrows.

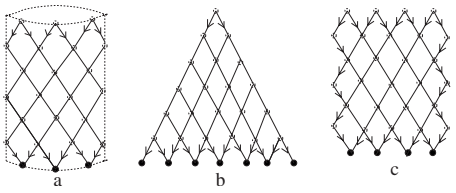

FIG. 8. Examples of 2D directed acyclic lattices. In (a) the lattice is periodic in the horizontal direction, being defined on a cylinder. In (b) and (c) the lattice is open in the horizontal direction.

One can define a simple stochastic process on the directed acyclic lattice by the Hamiltonian

$$H = 1 - \frac{1}{\mathcal{L}} \sum_I a_I, \tag{74}$$

and the $\mathcal{L}$ quadratic relations (69)–(71). Obviously the stationary state of the system is given by (73):

$$H\Phi = 0. \tag{75}$$

In order to find the spectrum of H, one uses the diagonal representations of the generators of a_I. The eigenvalues of a_I are obtained using the one-dimensional representations of the DAA. One starts with the boundary generators (this is the last row in the lattices of Fig. 7), solving Eqs. (71). The solutions are introduced in the quadratic relations (69) related to the sites in the next layer (this is the row before last in Fig. 8). The layer-by-layer procedure is repeated (we go against the arrows) up to when we have exhausted the lattice. The energy gap corresponding to the first excited state is obtained by taking for all the generators the eigenvalue 1 except for one generator belonging to the top of the lattice [there is only one in Fig. 8(b), and many in Figs. 8(a) and 8(c)] for which we take the eigenvalue $-\mu$. This gives an energy gap

$$E_1 = (1+\mu)/\mathcal{L}, \tag{76}$$

and we conclude that the system is always critical, and if the dimension of the directed acyclic lattice is D, the dynamic critical exponent is equal to $z=D$.

Before discussing two-dimensional directed acyclic lattices, we consider again a one-dimensional case in which the bulk sites in (69) are joined to two successive sites. The DAA is

$$a_i^2 = \alpha_1 a_{i+1}^2 + \alpha_2 a_{i+2}^2 + \beta_1 a_i a_{i+1} + \beta_2 a_i a_{i+2} + \gamma a_{i+1} a_{i+2},$$

$$a_{L-1}^2 = \alpha_2 + \beta_2 a_{L-1} + \gamma a_L + \alpha_1 a_L^2 + \beta_1 a_{L-1} a_L,$$

$$a_L^2 = \mu + (1-\mu) a_L. \tag{77}$$

We have shown, using the method presented in Sec. III, that the avalanches are again given by a random walker. We do not include the lengthy calculations in the paper. We would like to mention only an interesting observation. Let us take all the coefficients (77) zero except for γ. We get the deterministic algebra

$$a_i^2 = a_{i+1} a_{i+2} \quad (i = 0, 1, \ldots, L),$$

$$a_{L-1}^2 = a_L, \quad a_L^2 = 1, \tag{78}$$

and the stationary state is [see (73)]

$$\Phi = \prod_{i=1}^{L} \frac{1+a_i}{2}. \tag{79}$$

For simplicity, we take $L+1$ sites $(i=0,1,\ldots,L)$ with L even and assume that we have two particles on the site $i=0$ which trigger the avalanche. We also group the sites in pairs in the ground-state wave function (79). Using (78) and (73) we have

$$\begin{aligned} a_0^2 \Phi &= a_1 a_2 \prod_{i=1}^{L/2} (1+a_{2i-1})(1+a_{2i})/4 \\ &= \left(\frac{a_1 a_2}{4} + \frac{a_2 a_3 a_4}{4} + \frac{(1+a_2) a_3^2 a_4}{4} \right) \\ &\quad \times \prod_{i=2}^{L/2} \frac{(1+a_{2i-1})(1+a_{2i})}{4} \\ &\triangleq \left(\frac{1}{4} + \frac{a_3 a_4}{4} + \frac{a_3^2 a_4}{4} \right) \times \prod_{i=2}^{L/2} \frac{(1+a_{2i-1})(1+a_{2i})}{4}. \end{aligned} \tag{80}$$

There are three terms in the last equation. The first one gives with probability $1/4$ an avalanche of size 2. The second term, with probability $1/4$, has the same structure as the same equation for a lattice with $L-2$ sites. Using the identity

$$a_{2i-1}^2 a_{2i} \frac{(1+a_{2i-1})(1+a_{2i})}{4} = \frac{(1+a_{2i-1})(1+a_{2i}) a_{2i+1} a_{2i+2}}{4} \triangleq a_{2i-1}^2 a_{2i+2}, \tag{81}$$

we find that the last term in (80) describes three particles that "fly" to the boundary and leave the system. This occurs with probability $1/2$. Notice [see (78)] that $a_{L-1}^2 a_L = 1$.

To sum up, if L is large, one gets with probability $1/4^k$ an avalanche of size $2k$. This implies that with probability $1/3$ one gets finite avalanches. With a probability $2/3$ one gets "avalanches" of the size of the system. Let us mention that in two dimensions a similar deterministic model gives avalanches with long tails (exponent $\sigma_\tau = 3/2$) [12].

We have studied the behavior of avalanches in the two-dimensional directed cyclic lattice shown in Fig. 8(b) using the quadratic DAA algebra

$$\begin{aligned} a_{i,j}^2 &= \alpha(\mu a_{i+1,j}^2 + (1-\mu) a_{i,j} a_{i+1,j}) \\ &\quad + (1-\alpha)(\mu a_{i,j+1}^2 + (1-\mu) a_{i,j} a_{i,j+1}). \end{aligned} \tag{82}$$

The avalanches observed in the lattice in Fig. 8(b) coincide with those observed in the cylinder in Fig. 8(a) if the perimeter of the cylinder is larger than the size of the avalanche.

We did extensive Monte Carlo simulations for several values of the parameters in the DAA. We took only small values of μ to make sure that we do not get crossover effects like those described in Fig. 2. We have considered up to 1.2×10^8 avalanches of sizes up to $T=30\,000$. It is important to note that the estimate is smaller than the expected value.

The exponent σ_τ was obtained in several ways. A possible estimate is the value of $\omega = \sigma_\tau$ that makes

$$\left. \frac{\partial F(\omega, T)}{\partial T} \right|_{\omega = \sigma_\tau} = 0, \tag{83}$$

for $17\,500 < T < 30\,000$, where

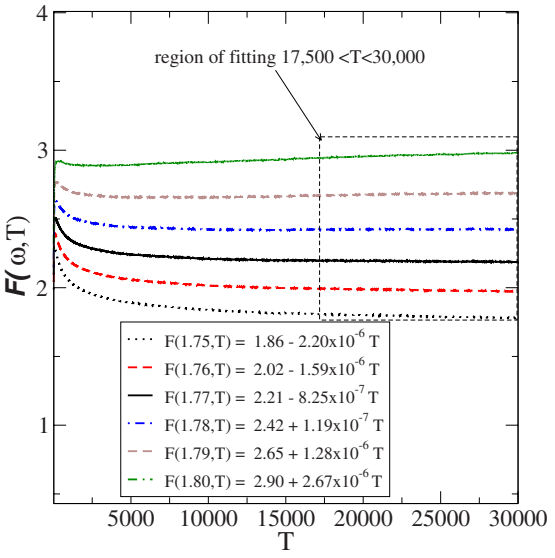

FIG. 9. (Color online) Function $F(\omega,T)$ as defined in (84) for some values of ω. This figure is for the stochastic model associated with (82) with $\alpha=1/2$ and $\mu=1/10$. In the inset we show the linear fit for the values of ω obtained from the data for $17\,500<T<30\,000$.

$$F(\omega,T)=T^{\omega-1}\int_{T}^{\infty}p(t)dt. \tag{84}$$

In Fig. 9 we show for $\alpha=1/2$ and $\mu=1/2$ the function $F(\omega,T)$ for some values of ω. The data suggest $1.77<\sigma_\tau<1.78$. The same calculations were done for $\alpha=1/2$, $\mu=1/10$, giving us $1.780<\sigma_\tau<1.785$, and also for the anisotropic lattice where $\alpha=1/4$, $\mu=1/2$, giving us $1.78<\sigma_\tau<1.79$. Our results indicate that the model in two dimensions belongs to a universality class where $\sigma_\tau=1.780\pm0.005$. We should keep in mind that in one dimension for $\mu=0.1$ and $T=30\,000$, one has obtained an estimate $\sigma_\tau(T)=1.49971$, quite close to and smaller than the correct value $3/2$. Previous Monte Carlo simulations [13] had larger errors. If one takes our results at face value, they contradict the theoretical predictions [14,15]. We cannot exclude, however, that larger values of T are necessary to get the ultimate value of σ_τ. We hope that our results motivate independent additional numerical studies in the future.

VI. CONCLUSIONS

Using directed acyclic lattices [5] we have defined directed Abelian algebras. The lattices can be in any dimensions. We attach a generator of the DAA to each site of the lattice. There are polynomial relations among the generators. A given DAA can depend on several parameters. The remarkable property of these algebras is that they are always semisimple.

For each DAA one can define a family of Hamiltonians acting on the regular representation of the DAA. These Hamiltonians give the time evolution of various stochastic processes. The vector space of the regular representation can be mapped in the vector space obtained by taking N states on each site of the directed acyclic lattice (N is the degree of the polynomial relations). In this way one obtains N-state Hamiltonians in an arbitrary number of dimensions.

It is easy to compute the whole spectrum for the family of Hamiltonians related to a given DAA. All one has to do is to find all the one-dimensional irreducible representations of the algebra. This is a purely algebraic exercise. Once the spectrum of the generators in the diagonal representation is known one can compute the spectrum of the Hamiltonians.

To find the eigenfunctions of the Hamiltonians, one has to solve a purely algebraic problem: one writes the one-dimensional representations in the basis of the regular representation. To find the ground-state wave functions corresponding to the stationary states one has to consider the irrep in which all the generators are equal to 1. The stationary states can easily be obtained for any Hamiltonian obtained from a DAA. The stationary states always have a product measure (there are no correlations) and depend on fewer parameters than the DAA. All the wave functions can probably be obtained. In a simple example (see Appendix A) we not only show how to obtain the whole spectrum but give also all the wave functions. They have a simple factorized form.

We have studied some simple Hamiltonians in which only the generators appear. For a simple mathematical reason, in the finite-size scaling limit, they are all gapless with a dynamic critical exponent $z=D$ (D is the number of dimensions of the lattice). There are many interesting time-dependent physical properties that are worth studying in these models, the simplest being the time evolution of local densities. We plan to look at these aspects of the models in the future. Instead we have studied the properties of avalanches. Each DAA together with the ground-state wave function of the Hamiltonian can define avalanches.

In one dimension and in a DAA algebra that conserves the number of particles, we have checked for two- and three-state models that one gets avalanches in the "random walk" universality class [7]. We have also studied the "composition" of avalanches. One has a depletion of particles at the position where the avalanche starts and an enrichment at the end of the avalanche. The Hamiltonian is gapless even if the DAA does not conserve the number of particles. This implies that one does not have SOC (the probability to have large avalanches decreases exponentially) in spite of the fact that the Hamiltonian is critical. One can complement this observation with another similar observation. Since we are in one dimension the stationary state of an N-state model can be seen as a spin model defined on the dual lattice. The spin model depends on many parameters (there is only one for $N=2$ corresponding to the temperature) and is not critical in spite of having a stochastic model which is critical. The opposite situation is already known [23]: a Hamiltonian having a gap drives the system to the critical (zero-temperature) spin system.

In two dimensions all we did is to check that for various choices of parameter one stays in the universality class described in [13–15]. In two dimensions, using large-scale Monte Carlo simulations, we have determined the probability to obtain large avalanches. We have measured the exponent σ_τ (usually denoted τ_t) and found a value that is close but not identical to the theoretical predictions [14,15]. More work is necessary to settle this problem.

ACKNOWLEDGMENTS

G. M. Nakamura participated in the initial stage of this work, and we thank him for further discussions. We thank D. Dhar, V. B. Priezzhev, and P. Pyatov for reading the manuscript and for their relevant suggestions. We thank A. Owczarek for providing us with the relation (49). This work has been partially supported by the Brazilian agencies FAPESP and CNPq.

APPENDIX A: SPECTRUM AND EIGENFUNCTIONS OF A HAMILTONIAN DERIVED FROM A QUADRATIC DIRECTED ABELIAN ALGEBRA

In Secs. II and III we discussed the quadratic Abelian algebra

$$a_i^2 = \mu a_{i+1}^2 + (1-\mu) a_i a_{i+1}, \quad i = 1,2,\ldots,L,$$

$$a_{L+1} = 1, \quad [a_i, a_j] = 0, \tag{A1}$$

and the Hamiltonian

$$H = \frac{1}{L}\sum_{i=1}^{L} (1 - a_i). \tag{A2}$$

In order to obtain the spectrum of H we have to find the representations of a_i in the diagonal representation. In order to find the wave functions one has to express the a_i in the regular representation. In the latter representation, the vector space is given by monomials of the a_j's (see Sec. II).

In the representation in which a_i are diagonal, the distinct eigenvalues x_i of a_i can be obtained recursively from the eigenvalues x_{i+1} of a_{i+1}:

$$(x_i - x_{i+1})(x_i + \mu x_{i+1}) = 0. \tag{A3}$$

Equation (A3) can be written as

$$x_i = (-\mu)^{\epsilon_i} x_{i+1} \quad (\epsilon_i = 0,1). \tag{A4}$$

This implies that the eigenvalues of a_{L-l} are

$$x_{L-l}(\epsilon_{L-l}, \epsilon_{L-(l-1)}, \ldots, \epsilon_L) = \prod_{j=0}^{l} (-\mu)^{\epsilon_{L-j}}, \tag{A5}$$

and are labeled by the $\epsilon_i = 0,1$ $(i = L, L-1, \ldots, L-l)$. In the 2^L representation of the algebra (A1), the eigenvalues of a_{L-l} are

$$x_{L-l}(\epsilon_1, \epsilon_2, \ldots, \epsilon_{L-l-1}, \epsilon_{L-l}, \epsilon_L) = \prod_{k=1}^{L-l-1} (1)^{\epsilon_k} \prod_{j=0}^{l} (-\mu)^{\epsilon_{L-j}}; \tag{A6}$$

except for a_1, they are degenerate.

We are going to show that in the regular representation, the factorized expression

$$\Psi(\epsilon_{L-l}, \epsilon_{L-l+1}, \ldots, \epsilon_L) = \prod_{m=0}^{l} [\mu + (-\mu)^{\epsilon_{L-m} - \sum_{j=0}^{m-1} \epsilon_{L-j}} a_{L-m}] \tag{A7}$$

is an eigenfunction of a_{L-l} corresponding to the eigenvalue (A5):

$$a_{L-l}\Psi(\epsilon_{L-l}, \ldots, \epsilon_{L-1}, \epsilon_L) = x_{L-l}(\epsilon_{L-l}, \ldots, \epsilon_{L-1}, \epsilon_L),$$

$$\times \Psi(\epsilon_{L-l}, \ldots, \epsilon_{L-1}, \epsilon_L). \tag{A8}$$

This implies that $\Psi_{\epsilon_1,\ldots,\epsilon_L}$ is an eigenfunction of all a_i $(i = 1,\ldots,L)$ corresponding to the eigenvalues (A6). In particular, if we take all the $\epsilon_i = 0$, one obtains the eigenvalue 1 for all the a_i which gives an eigenvalue zero for H [see (A2)] and the corresponding eigenfunction is, up to a normalization factor, equal to (16).

The spectrum of H is obtained by introducing the eigenvalues (A6) in (A2). Obviously (A7) is also an eigenfunction for all a_{L-j} $(0 < j < l)$.

Using (A6) one can compute all the eigenvalues of H (they are fixed by the values of the $\epsilon_i, i = L, L-1, \ldots, 1$). The corresponding eigenfunctions are given by (A7) with $l = L-1$. The proof of (A8) is by finite induction.

(a) (A8) is valid for $l = 0$. Using (A1) one has

$$a_L[\mu + (-\mu)^{\epsilon_L} a_L] = (-\mu)^{\epsilon_L}[\mu + (-\mu)^{\epsilon_L} a_L], \tag{A9}$$

in agreement with (A8).

(b) If (A8) is valid for l, it is valid for $l+1$ We have to check that a_{L-l-1} applied to $\Psi(\epsilon_{L-l-1}, \ldots)$ gives the eigenvalues (A6). One has

$$\begin{aligned} &a_{L-l-1}\Psi(\epsilon_{L-l-1}, \epsilon_{L-l}, \ldots, \epsilon_L) \\ &\quad = a_{L-l-1}[\mu + (-\mu)^{\epsilon_{L-l-1} - \sum_{j=0}^{l} \epsilon_{L-j}} a_{L-l-1}] \\ &\qquad \times \Psi(\epsilon_{L-l}, \epsilon_{L-l+1}, \ldots, \epsilon_L) \\ &\quad = x_{L-l-1}(\epsilon_1, \epsilon_2, \ldots, \epsilon_L) \times \Psi(\epsilon_{L-l-1}, \epsilon_{L-l}, \ldots, \epsilon_L), \end{aligned} \tag{A10}$$

where we have used (A1) and (A8).

We think that the factorized form of the eigenfunctions (A7) is a general property of stochastic models obtained from the DAA. It is a consequence of the representation theory of the DAA and not of a specific form of the Hamiltonians.

APPENDIX B: SEVERAL REPRESENTATIONS OF THE QUADRATIC DAA ALGEBRA (10)

We have to stress that, unlike the spectra of evolution operators, which are insensitive to the choice of the representations of the DAA algebras, the physical properties of the systems depend on the choice of the representation. For example, the existence or not of avalanches or even the universality classes of avalanches is not determined by the algebras but by their representations. Similarly, a redefinition of the linearly independent words $W(r)$ [see Eq. (1)] in the algebra changes the physics. For example, the shift $a_i \in a_i' + \gamma$ in the algebra (10) can make one of the coefficients p_2, p_3, or q_2 vanish, such a shift changes the physical process.

In order to clarify the importance of choosing different representations for the same algebra, we consider the simpler case of the quadratic algebra (25):

$$a_i^2 = \mu a_{i+1}^2 + (1-\mu) a_i a_{i+1} \quad (i = 1,2,\ldots L),$$

$$a_i a_j = a_j a_i, \quad a_{L+1} = 1. \tag{B1}$$

The expression of the generators in the 2^L regular representation used in Secs. II and III can be written in the following way:

$$a_i = I_{1,i-1} \otimes A_i, \tag{B2}$$

where $I_{i,j}$ is the 2^{j-i} unit matrix acting on the tensor product $V_i \otimes V_{i+1} \otimes \cdots \otimes V_j$, and V is a two-dimensional vector space. A_i is a 2×2 matrix, with elements acting on a 2^{L-i} vector space

$$A_i = \left(\begin{array}{c|cc} & 1 & a_i \\ \hline 1 & 0 & \mu A_{i+1}^2 \\ a_i & I_{i+1,L} & (1-\mu)A_{i+1} \end{array}\right). \tag{B3}$$

A second representation of the algebra is

$$a_i = I_{1,i-1} \otimes B_i \tag{B4}$$

where

$$B_i = \begin{pmatrix} 1-\alpha & \beta \\ \alpha & 1-\beta \end{pmatrix} \otimes B_{i+1}, \tag{B5}$$

with

$$\mu = \alpha + \beta - 1. \tag{B6}$$

There are no avalanches in this representation. A particle hitting the site i does not influence the site $i+1$.

A third representation is used in the totally asymmetric Oslo model [9–11]:

$$a_i = I_{1,i-1} \otimes C_i, \tag{B7}$$

where

$$C_i = \begin{pmatrix} (1-\alpha)C_{i+1} & \beta C_{i+1}^2 \\ \alpha I_{i+1,L} & (1-\beta)C_{i+1} \end{pmatrix} \tag{B8}$$

and $\mu=\alpha+\beta-1$.

The eigenvalues of a_i are the same for all three representations. The eigenfunction Φ

$$a_i \Phi = \Phi \quad (i = 1,2,\ldots,L) \tag{B9}$$

is also the same:

$$\Phi = \bigotimes_{i=1}^{L} \frac{1}{\alpha+\beta} \begin{pmatrix} \beta \\ \alpha \end{pmatrix}_i. \tag{B10}$$

To obtain representation (B3) one has to take $\alpha=1$ and $\beta=\mu$ in (B8).

In the representation (B4), taking into account (B10), the order of the lattice sites is lost due to the factorization of Φ. Topplings and virtual time cannot be defined.

One can repeat the calculations done in Sec. III and derive the properties of avalanches for the representation (B7). The results are a simple generalization of the previous results. Equation (43) stays unchanged with μ given by (B6) and the diffusion constant is $D=\alpha\beta/(\alpha+\beta)^2$. For $\alpha=1$, one recovers the results of Sec. III. The parameter μ in the algebra (B1) can take negative values. This is not the case if $\alpha=1$. The average density in the stationary state

$$\rho = \alpha/(\alpha+\beta) \tag{B11}$$

spans the interval $0 \leqslant \rho \leqslant 1$. The interval is smaller if $\alpha=1$.

[1] D. Dhar, Physica A **263**, 4 (1999).
[2] D. Dhar, Physica A **270**, 69 (1999).
[3] B. Tadic and V. Priezzhev, Phys. Rev. E **62**, 3266 (2000).
[4] F. Harari, *Graph Theory* (Addison-Wesley, Reading, MA, 1969).
[5] J. L. Gross and Y. Yellen, *Handbook of Graph Theory and Applications* (CRC Press, London, 2003).
[6] C.-C. Chen and M. den Nijs, Phys. Rev. E **65**, 031309 (2002).
[7] S. Maslov and Y.-C. Zhang, Phys. Rev. Lett. **75**, 1550 (1995).
[8] S. N. Majumdar and A. Comtet, J. Stat. Phys. **119**, 777 (2005).
[9] K. Christensen, A. Corral, V. Frette, J. Feder, and T. Jøssang, Phys. Rev. Lett. **77**, 107 (1996); M. Paczuski and K. E. Bassler, Phys. Rev. E **62**, 5347 (2000).
[10] G. Pruessner, J. Phys. A **37**, 7455 (2004).
[11] M. A. Stapleton and K. Christensen, J. Phys. A **39**, 9107 (2006).
[12] D. Dhar and R. Ramaswamy, Phys. Rev. Lett. **63**, 1659 (1989).
[13] R. Pastor-Satorras and A. Vespignani, J. Phys. A **33**, L33 (2000).
[14] M. Paczuski and K. Bassler, Phys. Rev. E **62**, 5347 (2000).
[15] M. Kloster, S. Maslov, and C. Tang, Phys. Rev. E **63**, 026111 (2001).
[16] F. C. Alcaraz and V. Rittenberg, J. Stat. Mech.: Theory Exp. (2007) P07009.
[17] A left I ideal of an algebra A is a subspace of A such that $aX \in I$ for all $a \in A$ and $X \in I$.
[18] S. Redner, *A Guide to First-Passage Processes* (Cambridge University Press, London, 2001).
[19] J. Theiler, Phys. Rev. E **47**, 733 (1993).
[20] A. Barrat, A. Vespignani, and S. Zapperi, Phys. Rev. Lett. **83**, 1962 (1999).
[21] A. M. Povolotsky, V. B. Priezzhev, and Chin-Kun Hu, J. Stat. Phys. **111**, 1149 (2003).
[22] A. Owczarek (private communication).
[23] F. C. Alcaraz, M. Droz, M. Henkel, and V. Rittenberg, Ann. Phys. (N.Y.) **230**, 250 (1994).